

**Assessing the simulation of snowfall at Dumont d'Urville,
Antarctica, during the YOPP-SH special observing campaign**

Journal:	<i>QJRMS</i>
Manuscript ID	QJ-22-0102
Wiley - Manuscript type:	Research Article
Date Submitted by the Author:	29-Apr-2022
Complete List of Authors:	Roussel, Marie-Laure; Laboratoire de Météorologie Dynamique, Ecole Polytechnique - IPP Genthon, Christophe; Laboratoire de Météorologie Dynamique, Sorbonne Université Vignon, Etienne; Laboratoire de Météorologie Dynamique, Sorbonne Université Bazile, Eric; Centre National de Recherches Météorologiques, GMAP, Météo-France Agosta, Cécile; LSCE, IPSL, CEA-CNRS-UVSQ, Université Paris-Saclay berne, alexis; EPFL, Swiss Federal Institute of Technology in Lausanne Durán-Alarcón, Claudio; CESAM, Department of Physics, University of Aveiro Wiener, Valentin; Laboratoire de Météorologie Dynamique, Sorbonne Université Dufresne, Jean-Louis; Laboratoire de Météorologie Dynamique, Sorbonne Université Claud, Chantal; Laboratoire de Météorologie Dynamique, Ecole Polytechnique
Keywords:	Observations < 1. Tools and methods, YOPP, snowfall, Antarctica, meteorology, precipitation radar
Country Keywords:	AAA - No country

1
2 **Assessing the simulation of snowfall at Dumont d'Urville, Antarctica, during the YOPP-SH**
3 **special observing campaign**
4

5 Roussel M.-L., Genthon C., Vignon E., Bazile E., Agosta C., Berne A., Durán-Alarcón C., Wiener
6 V., Dufresne J.-L., Claud C.
7



On the East Antarctic coast in Adélie Land, Dumont d'Urville station YOPP supersite is a favorable place to study regional meteorological phenomena despite the extreme conditions prevailing there. The YOPP campaign during the 2018-2019 austral summer made it possible to combine significant means of measurement as well as numerical simulations, giving rise to an unprecedented local study of snowfall, at the surface and at altitude highlighting the different performances of the models.

For Peer Review

1
2
3
4
5
6
7
8
9
10
11
12
13
14
15
16
17
18
19
20
21
22
23
24
25
26
27
28
29
30
31
32
33
34
35
36
37
38
39
40
41
42
43
44
45
46
47
48
49
50
51
52
53
54
55
56
57
58
59
60



59x49mm (300 x 300 DPI)

ORIGINAL ARTICLE

Journal Section

Assessing the simulation of snowfall at Dumont d'Urville, Antarctica, during the YOPP-SH special observing campaign

Marie-Laure Roussel¹ | Christophe Genthon¹ | Etienne Vignon¹ | Eric Bazile² | Cécile Agosta³ | Alexis Berne⁴ | Claudio Durán-Alarcón⁵ | Valentin Wiener¹ | Jean-Louis Dufresne¹ | Chantal Claud¹

¹Laboratoire de Météorologie Dynamique, Institut Pierre-Simon Laplace, Sorbonne Université/CNRS/École Polytechnique - IPP, Paris, France

²Centre National de Recherches Météorologiques, GMAP, Météo-France, Toulouse, France

³Laboratoire des Sciences du Climat et de l'Environnement, IPSL, CEA-CNRS-UVSQ, Université Paris-Saclay, Gif-sur-Yvette, France

⁴Environmental Remote Sensing Laboratory, Swiss Federal Institute of Technology in Lausanne, Lausanne, Switzerland

⁵CESAM - Centre for Environmental and Marine Studies, Department of Physics, University of Aveiro, Aveiro, Portugal

Correspondence

Marie-Laure Roussel, Laboratoire de Météorologie Dynamique, Ecole Polytechnique, Palaiseau, 91128, France
Email: marie-laure.roussel@lmd.polytechnique.fr

Funding information

CALVA, French Polar Institute, Grant Number: 103; EECLAT, CNES/CNRS

The performance of a set of atmospheric models and meteorological reanalyses in the representation of precipitation days in Antarctica is assessed using benchmark ground-based observations such as a snow gauge and a Micro Rain Radar during the Year Of Polar Prediction Special Observing Period at Dumont d'Urville (November 2018 - February 2019), East Antarctic coast. The occurrence of precipitation observed is mostly well predicted but the number and intensity of days with snowfall are overestimated by the models. This is reflected by high values of bias, probability of detection and false alarm ratios, in particular for reanalyses, due to numerous simulated precipitating days. The Heidke skill score shows the overall great contribution of the models in the forecasting of precipitating days, and the best performances are achieved by numerical weather prediction models. The chronology is better represented when the models benefit from the data assimilation of in-situ observations, such as in reanalysis or weather forecasting models. Precipitation amounts at the surface are overestimated by most of the models. In addition, data from the

ground-based radar make it possible to evaluate the representation of the vertical profiles of snowfall. Thus it is possible to see when small surface error is due to excessive sublimation in the atmospheric boundary layer compensating for overly strong precipitation flux in the mid and low troposphere. Therefore the need to expand the measurement of precipitation across the atmospheric column using radars is highlighted, in particular in Antarctica where the cold cloud microphysics is poorly known and observations are particularly rare.

KEYWORDS

Antarctica, snowfall, YOPP, observations, precipitation radar, meteorology

1 | INTRODUCTION

The Antarctic continent - 14 million square kilometers-wide and almost totally covered by ice - is the largest continental reservoir of water on Earth. Assessing the future evolution of the inlandis mass balance is therefore critical in the framework of climate change. The surface mass balance (SMB) of the Antarctic ice sheet is the net snow accumulation at its surface. The SMB is mainly fed by precipitation whereas surface loss is due to surface - and drifting - snow sublimation and runoff of melted water to the ocean. The main focus of this study is the Antarctic precipitation, which is expected to increase by the end of the century according to climate scenarios from the Coupled Model Intercomparison Project (CMIP) ([Palerme et al., 2017], Vignon et al. [2021]). When it comes to precipitation in Antarctica, the different climate models are in great disagreement. While there was no significant improvement between the CMIP5 and CMIP6 results (Roussel et al. [2020]), the reliability of the precipitation scenarios is questionable and there is a urgent need to evaluate and improve the models. The evaluation of models requires reference observational data and a well defined evaluation set-up. Satellite data are very useful for the study of the atmospheric column : thanks to the measurements of the Cloud Profiling RADAR (CPR) onboard the CloudSat satellite the first model-free surface snowfall climatology over Antarctica have been made (Palerme et al. [2014], Palerme et al. [2019]) then further expanded by adding the vertical component (Lemonnier et al. [2020]). This dataset enables to assess some spatial and temporal characteristics of the vertical distribution of antarctic precipitation. But there are limitations : the revisit time is quite long, the CPR does not give measurements below 1200 meters - while it is often below this altitude that the most intense snowfall occurs and especially in the lower layers of the atmosphere that sublimation by katabatic winds takes place (Grazioli et al. [2017b], Durán-Alarcón et al. [2019], Vignon et al. [2019b]) - then it was only operational between 2007 and 2010.

The Year Of Polar Prediction in the Southern Hemisphere (YOPP-SH) campaign which took place between 2017 and 2019 is a unique opportunity to carry out an in-depth evaluation of models thanks to the large amount of observational data collected and the simulations provided by climate and weather prediction centers. The YOPP was part of the Polar Prediction Project (PPP) of the World Weather Research Program (WWRP) initiated by the World Meteorological Organisation (WMO) whose main objective was i) to improve the meteorological observations at the poles, ii)

to enhance the prediction capabilities of Numerical Weather Prediction (NWP) models at high-latitudes, iii) to advance our understanding of the dynamical and physical processes that govern the polar climates and their interactions with mid- and low-latitudes (Bromwich et al. [2020]). A Special Observation Period (SOP) took place at both poles, with a particular focus at so-called *Supersites* - i.e. specific points of interest with an enhanced observational system - such as the french scientific station Dumont d'Urville (DDU) in coastal Adélie Land, East-Antarctica (see section 2.1 for the description of the site). At this station, the frequency of observations was increased and simulations have been made especially to cover the campaign period between November 2018 and February 2019. Beyond WMO standards, the station is also equipped with a Micro Rain RADAR (MRR) which is very useful for evaluating the vertical structure of precipitation. Although the ground-based MRR data only make it possible to evaluate the precipitation modeled at a specific location, they provide information along the vertical and in particular on the lower layers of the atmosphere, and with a very fine temporal resolution (Lemonnier et al. [2021], Vignon et al. [2019a]). While it is common-practice to evaluate the surface precipitation as simulated by models, this approach misses the relative importance of certain physical processes in the atmospheric column such as sublimation - which takes place above the surface and impacts substantially the final result at the ground - especially in case of katabatic winds (Grazioli et al. [2017b]) which are prevailing at DDU. Thus an outlook of the atmospheric column is considered in this work especially thanks to the MRR.

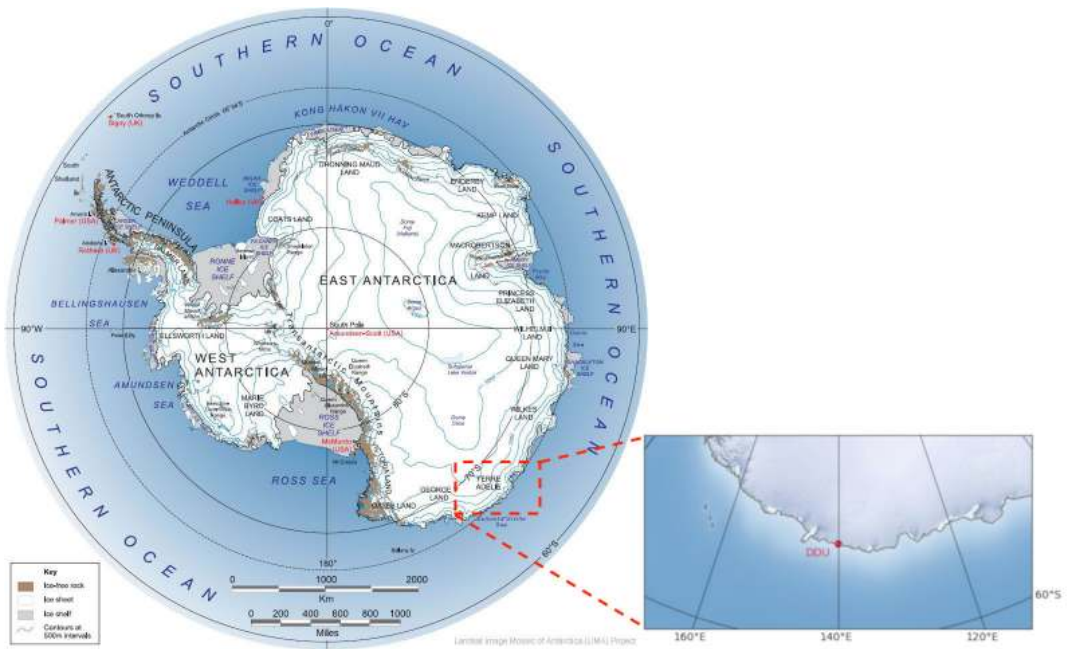
In this study we focus on two operational analyses, two reanalyses and two climate models including a global atmospheric model and a regional one in the vicinity of the DDU station : ARPEGE (Action de Recherche Petite Echelle Grande Echelle) outputs of the operational NWP model with a zoom focused on the Dome-C - about 1000 kilometers from DDU, IFS (Integrated Forecast System) outputs of the operational NWP model, LMDZ zoomed on DDU, MAR, ERA5 and MERRA2 reanalysis (see Section 2.3 for a complete description of the models). The objective is to evaluate the performance of the different types of models. To this end, a comparison with the observational data of the occurrences and quantities of snowfall flux at the surface and along the vertical is carried out. A detailed presentation of the observations and model output data used in this work is given in Section 2. Section 3 presents the meteorological conditions at the Dumont d'Urville station during the YOPP campaign, with a particular focus on days with snowfall. Then, the results of the evaluation of the models are given in Section 4. Section 5 closes the paper with a general discussion and conclusions.

2 | DATA & METHODS

2.1 | Presentation of the DDU station

The Dumont D'Urville (DDU) station is located at latitude 66.663 S and longitude 140.0 E (local time : UTC + 10H) on Petrel's Island at about five kilometers off the coast of Adélie Land (see Figure 1). This is a privileged point for observation, in particular thanks to the many technical means which are deployed there. DDU is located in a region affected by the katabatic winds that are very frequent on the East Antarctic coast. It is a coastal site that receives a significant amount of precipitation. Thus its location and the presence of its operational meteorological station (König-Langlo et al. [1998]) since 1956 have motivated various studies and have led to some scientific missions concerning the study of precipitation, such as the APRES3 (Antarctic Precipitation, Remote Sensing from Surface and Space) project that ran from 2015 to 2019 and during which instruments (including a MRR and a snow gauge) were deployed at the station to measure snowfall quantities (Genthon et al. [2018]). However, it is difficult to compare the observations at this site to the models because of the strong land-sea contrasts - with masks - as well as the altitude of the surface. Nevertheless, it has been chosen to be a *supersite* during the southern hemisphere part of the YOPP campaign from

1
2 november of 2018 to february of 2019.



25 **FIGURE 1** Map of Antarctica and the Southern Ocean produced by the LIMA (Landsat Image Mosaic of Antarctica) Project
26 (left) zoomed on the East coast (right). Blue lines indicates the topography of Antarctica. Research stations are in red text,
27 ice-free rock areas in brown, ice shelves in gray and names of the major ocean water bodies in blue uppercase text (USGS
28 [2022]). The DDU station is indicated by a red dot.

32 | 2.2 | Ground-based observations and satellite remote-sensing measurements

36 | 2.2.1 | Snow gauge

39 Surface snow precipitation is measured using a OTT PLUVIO2 snow gauge (Grazioli et al. [2017a], Genthon et al.
40 [2018]). The gauge measures the mass of snow falling in a bucket placed on a scale that detects mass changes. It
41 is worth emphasizing that this system cannot distinguish between the accumulation of snow due to snowfall from
42 blowing snow entering the gauge. A wind shield reduces the undercatch of airborne falling particles but the weather
43 conditions at DDU are so extreme (severe gusts occasionally reaching $180\text{km}\cdot\text{h}^{-1}$, wind direction changes and turbu-
44 lences) that recorded measurements may be affected by artifacts. Here phantom events due to vibration and blowing
45 snow were removed with MRR data using the method of Grazioli et al. [2017a]. However, phantom mass measure-
46 ments due to strong wind events occurring simultaneously with snowfall (both measured by the snow gauge and the
47 MRR) cannot be corrected.

2.2.2 | MRR

The METEK MRR is a 24.3GHz K-band radar and its half-power beamwidth is 2° - corresponding to a diameter of 50 meters at 3000 meters above ground level. It was installed in a radome in November 2015 and provides since then vertical profiles of reflectivity and Doppler velocity with a vertical resolution of 100 meters up to 3 kilometers. Data have been processed following the processing chain for snow hydrometeors developed by Maahn and Kollias [2012]. Snowfall rates are computed every 10 seconds using the Z-S relationship derived in Grazioli et al. [2017a] for DDU conditions, which was calibrated for the same season that the YOPP-SH campaign was carried out. The first valid range gate is at 300 m a.g.l., which can be compared to the measurements of snowfall at the surface by the snow gauge. Nevertheless, as this law has been developed for the lowest radar gate (300 meters) its parameters are calibrated for certain types of particles which varie with altitude, from 1000 meters and in particular above 2000 meters, because of the different properties of hydrometeors. The confidence interval of the parameters of the law given in Grazioli et al. [2017a] then makes it possible to evaluate an uncertainty range on the snowfall profile (see Figure 8).

2.2.3 | Weather sensors and monthly climatological tables

The scientific station of Dumont d'Urville is instrumented with an operational meteorological station operated by the french weather service Meteo-France according to the World Meteorological Organization (WMO) standards. Standard measurements of meteorological variables (2-m temperature and humidity, 10-m wind, and surface pressure) are collected all year long at a 1-min temporal resolution. Radioprobes are launched daily and up to 3 times a day during the YOPP SOP. Visual observations of present weather (cloud cover, cloud type, precipitation type) are also made every day at 00, 03, 06, 09 and 21 UTC (no observation during local "night"). Daily summaries are reported in climatological monthly tables (TCM). It is worth noting that visual observations are not completely objective and may also be tainted by errors. In the automatic dataset, there is also a code (see Table S.2) which gives information about the present weather. It is particularly interesting because it informs about the type of precipitation which is visually observed during the past hour.

2.3 | Data from atmospheric models and meteorological reanalyses

Details of each models are given in this section. General information concerning the horizontal, vertical and temporal resolutions of the datasets used is given in Table 1. Among all the weather forecasting models, atmospheric circulation models and reanalyses available on Antarctica, we have chosen to analyze only 6 of them, which are well representative of the area studied and whose data are freely accessible. Since we simultaneously study outputs of real forecasting models (with a forecasting time step), quantities calculated from analyses of forecasting models, as well as models nudged by continuous reanalyses, it is necessary to pay attention to the temporal dimension of the data compared. The daily average results of the different models (computed using UTC times) will be called "forecasts" hereinafter, whether they are predictions from weather forecasting models or outputs from nudged climate models. For ARPEGE and IFS, the daily average forecast for one day will be calculated from all the time steps of the forecast of this day (starting at 00H). However for climate models and reanalyses there is no forecasting time step. The daily average is therefore calculated respectively from all the hourly (or tri-hourly) results of the simulation and analysis of the day.

TABLE 1 Characteristics of models outputs used in this work. Daily outputs (averages or cumulative values for precipitation) are used in the analysis to match the various models resolutions. For the vertical description, the number of levels and the altitude of center of the first and the last levels are given.

Model (reference)	Horizontal resolution	Vertical resolution	Temporal resolution of the output
ARPEGE-SH (Pailleux et al. [2014])	variable (zoom on Dome-C) near DDU : 10km	106 levels 10-75000m	1 hour (instantaneous)
ECMWF-OPER (ECMWF [2021])	18km	91 levels 9-80000m	1 day (average)
LMDZ + ERA-Interim nudging (Hourdin et al. [2020])	variable (zoom on DDU) near DDU : 50km	95 levels 9-87000m	1 hour / 1 day (average)
MAR + ERA5 nudging (Kittel et al. [2021])	35km	24 levels 2-15000m	1 day (average)
ECMWF-ERA5 (Hersbach et al. [2020])	18km	137 levels 9-80000m	1 hour (instantaneous)
MERRA2 (Gelaro et al. [2017])	55km	73 levels 100-80000m	3 hours (average)

2.3.1 | Simulations from Numerical Weather Prediction models: ARPEGE and IFS

ARPEGE-SH

ARPEGE (Action de Recherche Petite Echelle Grande Echelle) is a global hydrostatic model of NWP (Pailleux et al. [2014]). It is developed by Météo-France and used for weather forecasting. The model is sometimes used for Antarctic studies (Ricaud et al. [2020]). The cloud microphysics of ARPEGE has four pronostic variables (cloud ice and water, solid and liquid precipitation). ARPEGE-SH is the dedicated configuration built for the YOPP-SH campaign. This specific configuration of the operational model is used with a higher resolution (around 7.5km) over Antarctica (with a zoom centered on Dome-C, 123.3E 75.1 S, East Antarctic Plateau) than for the NWP operational version over France (see Table 1). A 4DVar assimilation was performed every 6 hours with the *in-situ* (radiosondes, aircrafts, ground-based stations, buoys and ships datasets) and satellite observations used by the operational version of ARPEGE. We focused only on the 1-day forecasts initialized at 0:00 UTC (10:00 LT) every day for the DDU supersite for which two nearest grid points have been extracted for ARPEGE (one point is over sea and one is over land).

IFS

The IFS (Integrated Forecasting System) model is a global NWP model developed at the European Centre for Medium-range Weather Forecasts (ECMWF). Its cloud microphysics scheme is described in ECMWF [2021]. The ECMWF contribution in the YOPP dataset archive consists of two different products that have been made available for the whole campaign : one operational ensemble medium-range forecast - performed at around 18 kilometers resolution with hourly outputs of selected meteorological fields from the IFS - and one dedicated short-range research run which

is similar to the operational control forecast of the ensemble run. In this work we evaluate the second product. The YOPP dataset can be founded on the ECMWF website (ECMWF [2017]) and it is presented in Bauer et al. [2020].

2.3.2 | Reanalyses datasets : ERA5 and MERRA2

ERA5

ERA5 is a global reanalysis of the atmosphere produced by the ECMWF based on the IFS model (version CY41R2) and its data assimilation system (Hersbach et al. [2020]). Numerous atmospheric, land and oceanic variables are computed on a 30 km resolution grid. Since 2019, ERA5 supercedes the previous ERA-Interim reanalyses dataset - for the whole time period since 1979. We also computed the instantaneous solid precipitation fluxes by applying the methods used in line in the IFS model - detailed in the description of the model (see S.2). However, this method to retrieve solid precipitation fluxes has uncertainties because the computation is not made at the native time step of the model.

MERRA2

The Modern-Era Retrospective analysis for Research and Applications, (MERRA) is a global reanalysis based on the Goddard Earth Observing System Version 5 (GEOS5) Earth System Model - which is a set of atmospheric, ocean and land model components developed by the Global Modeling and Assimilation Office (GMAO) of the National Aeronautics and Space Administration (NASA) - and with an advanced assimilation system including several *in-situ* and space-based meteorological observations. Since 2016, the second version MERRA2 (Gelaro et al. [2017]) supersedes the original MERRA dataset, providing data from 1980 on a 50 kilometers resolution grid. The dataset used in this study can be founded on the NASA Goddard Earth Sciences (GES) Data and Information Services Center (DISC) website (GMAO [2015]).

2.3.3 | Simulations from climate models: LMDZ and MAR

LMDZ

The LMDZ General Circulation Model is the atmospheric component of the Institut Pierre Simon Laplace (IPSL) - Earth system Coupled Model (Boucher et al. [2020]), historically and still actively used in CMIP. LMDZ has been long used for Antarctic climate studies (e.g. Genthon et al. [2002], Krinner et al. [2019]) and its physics has been evaluated and improved for Antarctic conditions, especially regarding boundary-layer (Vignon et al. [2019b]) and precipitation processes (Lemonnier et al. [2021]). The 6th and last version of the model that is used in this paper is presented in Hourdin et al. [2020] and the cloud and precipitation parametrization is thoroughly described in Madeleine et al. [2020]. For this study, we have carried out LMDZ simulations with the zooming capability of the model (see Table 1) in a nudged mode, as described Vignon et al. [2018]. The zoom consists in stretching the horizontal Arakawa-C 64 x 64 grid in both latitude and longitude in order to obtain a refined domain of 62 km x 62 km centered on DDU (see Figure S.1). A nudging on the temperature, humidity, zonal and meridional wind component with ERA-Interim reanalyses is applied outside the zoom region with a time-scale of 6 hours. Therefore, the subcomponents of the physics of the model can be evaluated apart from likely deficiencies in the representation of the large-scale atmospheric dynamics and makes it possible to perform a chronologic comparison with in situ data from the DDU observatory.

MAR

The Regional Atmosphere Model (MAR) is a limited-area regional model (Gallée [1995]). It has been specifically developed for polar regions and is thoroughly used in Antarctic studies (Agosta et al. [2019], Kittel et al. [2021], Amory

1 et al. [2021]). In this study, we used MAR version 3.11, as in Kittel et al. [2021], solving conservation equations
2 for five water species : snow particles, cloud ice crystals, rain drops, cloud droplets, and specific humidity (Kessler
3 [1995], Gallée [1995]). Airborne particles can be advected vertically from one atmospheric layer to another and con-
4 tribute through sublimation to the heat and moisture budget of the atmosphere (Agosta et al. [2019], Le Toumelin
5 et al. [2021]). Limited area requires forcing at the limits of the domain. MAR simulations used in this study are made
6 with a ERA5 nudging (from mid-troposphere to the top) on a grid of 6000 x 7000 kilometers (see Table 1 for details)
7 around the Antarctic continent.
8
9

10 11 12 13 14 **2.4 | Evaluation methodology**

15
16
17
18
19 To assess the quality of prediction of the six simulations and reanalyses we evaluate both the accuracy of the timing
20 of the precipitation occurrences and of the amount of snowfall during the campaign. At surface, the reference used
21 for total snowfall is the data from the snow gauge OTT PLUVIO2. The surface solid precipitation was extracted from
22 modeling datasets to perform the surface comparison. Along the vertical, the reference observational dataset is that
23 from the MRR, which is compared to the profiles of solid precipitation fluxes from the simulations and reanalyses.
24 As all the simulations and reanalyses are not available with hourly timesteps, we chose to make the comparison at
25 the daily time scale. Also we choose to consider PLUVIO2 as the daily surface reference to keep a single framework
26 between comparisons of occurrences and quantities. Thus daily observed snowfall accumulations - according to the
27 reference selected (PLUVIO2 for surface snowfall or MRR for snowfall on the vertical column) - are considered as
28 individual events and compared to those that have been predicted.
29
30
31
32
33

34 **2.4.1 | Grid point selection**

35
36
37
38
39 Three grid points (see Table 2 - note that non zero altitudes on ocean surface are due to the spectral representation of
40 the surface geopotential - and Figure 2 - note that some points are overlapping) were selected for each model studied
41 : the closest to the real coordinates of the DDU station, the closest fully oceanic grid point (i.e. the closest with 100%
42 of type "sea") and the closest fully terrestrial grid point (i.e. the closest with 100% of type "land"). For ARPEGE and
43 MAR, only two points are extracted because the closest point is already fully oceanic or terrestrial. A preliminary
44 comparison of the three grid points, based on surface and vertical snowfall amounts (see Table S.1), made it possible
45 to assess that the most accurate representation of snowfall amounts is the one of the closest grid point regardless of
46 the surface type for most of the outputs. Therefore we only present and analyse the detailed comparison between
47 the simulations or reanalyses to the observations for the closest grid point whatever the nature of surface.
48
49
50
51
52
53
54
55

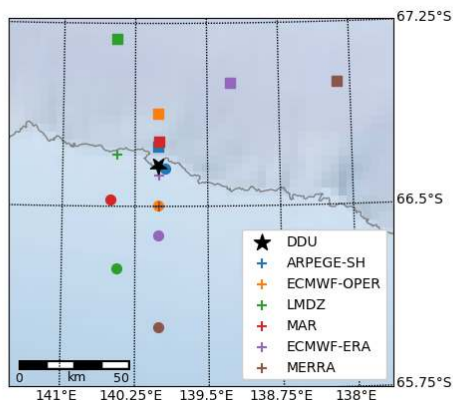


FIGURE 2 Location of the models grid points. Crosses, circles and squares respectively indicate the nearest, oceanic and terrestrial grid points. Real coordinates of DDU are indicated by a black star. The grey line represents the actual coastline.

TABLE 2 Grid points information (coordinates, distance from DDU and altitude) of modeling datasets

Model / Grid point	Nearest	Nearest fully oceanic	Nearest fully terrestrial
ARPEGE-SH	Fully oceanic	66.652 S 139.9 E	66.743 S 140.004 E
		3km, 91m	9km, 1617m
ECMWF-OPER	66.625 S 140.0 E	66.5 S 140.0 E	66.875 S 140.0 E
	4km, 108m (28% land)	18km, -16m	24km, 603m
LMDZ	66.711 S 140.433 E	65.756 S 140.433 E	67.180 S 140.433 E
	20km, 2027m (57% land)	103km, 0m	60km, 10796m
MAR	Fully terrestrial	66.523 S 140.492 E	66.760 S 139.994 E
		34km, 0m	11km, 321m
ECMWF-ERA5	66.625 S 140.0 S	66.375 S 140.0 E	67 S 139.25 E
	4km, 118m (43% land)	50km, -18m	32km, 1063m
MERRA2	66.5 S 140 E	66 S 140 E	67 S 138.125 E
	18km, 1892m (34% land)	74km, 0m	90km, 11184m

2.4.2 | Thresholding and classification of days with snowfall

Precipitation events are considered at the daily time scale. In order to filter the instrumental noise as well as spurious numerical precipitation in models, it is necessary to determine precipitating days that are considered as significant or non-negligible. The snow gauge having already been filtered out using data from the lowermost MRR gate data, it is considered that any precipitating day with more than 0 mm is not negligible. Also, the manufacturer's manual indicates

1
2 that a native threshold of 0.1mm per hour is already taken into account in the raw results of the snow gauge. Across
3 the vertical atmospheric column, it can happen that values measured by the MRR are masked. They are echoes filtered
4 out by the processing algorithm depending on a threshold set to distinguish if the reflectivity is strong enough to be
5 considered. We then choose to consider that these cases of undefined values are non-precipitating days - given that
6 there are no zero values in the MRR dataset - except for the cases where the quality variable indicates an absence
7 of data. It is also necessary to consider that the sensitivity of the MRR decreases vertically because electronic and
8 thermal noise increase with altitude. By construction, the minimum reflectivity detectable by the MRR increases with
9 the square of the distance from the instrument. To take this into account, it has been chosen to filter out the data
10 according to the value of the Signal to Noise Ratio (SNR), which guarantees that a clearly visible signal is kept. Thus
11 a minimal value of SNR is considered in order to remove precipitation measurements that are strongly impacted by
12 noise before any comparisons. The choice of this threshold as well as its impact on the observations are detailed in
13 S.6. In the models comparisons (not in models statistics), we choose a threshold of 0.28mm per day. This criterion
14 has been established by Palermé et al. [2014] to optimize the agreement between observations (CloudSat in Palermé
15 et al. [2014], MRR here) and the numerical simulations, based on a comparison between ERA-Interim and CloudSat
16 datasets. We choose to use this threshold by coherence with the preceding works and in order to be able to extend
17 this study thereafter to a comparison of the reanalyses of the ECMWF with instruments such as that carried on board
18 CloudSat (during its operating period) or the one planned for the future EarthCare satellite platform.

19
20 We apply this threshold on the whole vertical by considering that the numerical error in the models does not
21 depend on the altitude. In order to analyze their occurrence, we classify days with snowfall at the surface into six
22 quantitative classes : intense with 10 mm or more per day, medium with 5 to 10 mm per day, small with 1 to 5 mm
23 per day, very small with 0.28 to 1 mm per day, negligible with less than 0.28 mm per day, and null event with exactly
24 0 mm per day. This last category has very different results depending on the model conventions to treat the absence
25 of precipitation (see Figure 5) or low precipitation values - some models may have non-zero values due to numerical
26 accuracy and rounding errors.

27 28 29 **2.4.3 | Evaluation of the detection of snowfall occurrence**

30
31 A contingency table is used to qualify the quality of the simulations and reanalyses results regarding daily occurrence
32 of snowfall regardless of quantity, except the minimal threshold of 0.28mm per day for daily snowfall that is chosen to
33 distinguish days with precipitation from those without (or negligible) precipitation in the measurements or numerical
34 outputs. A dichotomous result based on the threshold mentioned above is attributed for each day and at each
35 level (for the comparison with the MRR dataset - considering the closest model level to the level of the MRR). In
36 the special case of the inter-comparison between observations (see Figure S.3), the minimum threshold retained to
37 consider precipitating days is 0mm per day. An additional comparison has been made between visual and instrumental
38 observations of surface snowfall occurrences (see S4) showing a good agreement between human observations and
39 data from the snow gauge. In this study, the following basic scores are analysed to investigate the quality of the
40 predicted precipitation occurrence, with H, FA, M and CR being respectively Hits, False Alarms, Misses and Correct
41 Rejects :

- 42
43
44 – Bias (B): $Bias = \frac{H+FA}{H+M}$ Ratio of forecasted days with snowfall on observed ones. If $B > 1$ (respectively $B < 1$),
45 then the model over-estimate (respectively under-estimate) the occurrence. The perfect score is 1.
46 – Probability Of Detection (POD): $POD = \frac{H}{H+M}$ Proportion of hits among forecasted days with snowfall. It is
47 sensitive to hits but ignores false alarm. The perfect score is 1.
48
49
50
51
52
53
54
55

- 1
2
3
4
5
6
7
8
- False Alarm Ratio (FAR) : $FAR = \frac{FA}{H+FA}$ Ratio of predicted days with snowfall on unobserved ones. The perfect score is 0.
 - Heidke Skill Score (HSS) : $HSS = \frac{2*(H*CR-FA*M)}{(H+M)*(M+CR)+(H+FA)*(FA+CR)}$ It measures the performance of forecasting against a random forecast. A negative value indicates that the random forecast is better. 0 means that the model has no particular skill. The perfect value is 1.

9 | METEOROLOGICAL CONDITIONS IN ANTARCTICA AND AT DUMONT D'URVILLE DURING THE YOPP CAMPAIGN

3.1 | Standard meteorological variables during the YOPP campaign

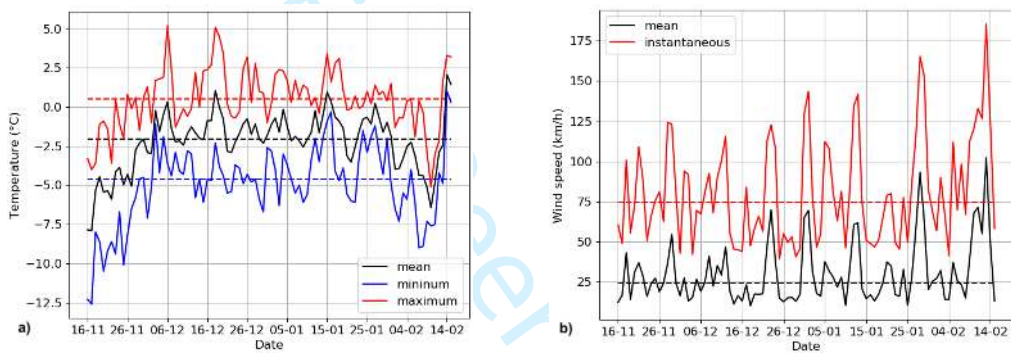
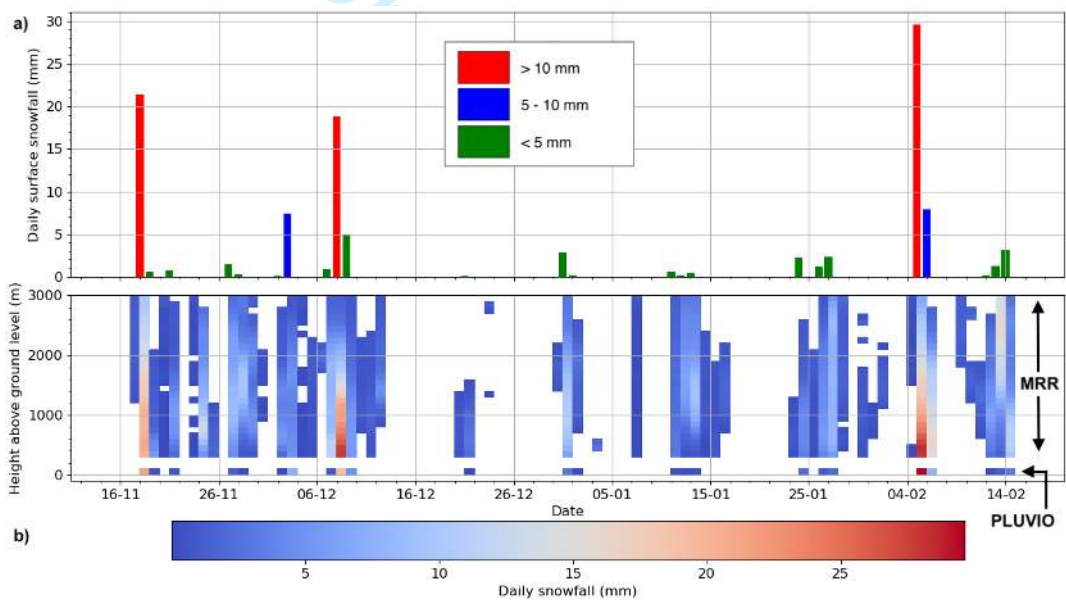


FIGURE 3 a) Time series of the daily mean of hourly 2-m temperature in degrees Celsius (minimum, maximum and mean temperatures are respectively in solid blue, red and black lines). b) Time series of the daily mean of hourly 10-m wind speed in $\text{m}\cdot\text{s}^{-1}$ on the right (mean and instantaneous wind speed are respectively in solid black and red lines) during the YOPP-SH campaign measured by the Météo-France sensors at the DDU station (November 2018 - February 2019). Median values are illustrated in dashed lines.

The climate at DDU station is milder than on the continent but very windy. As it is located on the east coast where the altitude is close to sea level, the influence of synoptic systems transiting over the Southern Ocean is not negligible as well as the warming by the ocean (König-Langlo et al. [1998]). The temperatures rarely fall below -30°C and the maximum can exceed 0°C . Winds at DDU are mostly katabatic winds forming on the slope of the continent with an easterly direction (Vignon et al. [2019b]). Their strength can be particularly strong when the synoptic conditions favor a plateau-to-ocean pressure gradient force (Bromwich and Parish [1998]). The direction - from South East to South at DDU - is determined by the slope and deviated by the force of Coriolis. The main direction of the winds at DDU during YOPP-SH is between 90 and 130 degrees, which corresponds to katabatic winds. It is more frequent during the inter-seasons and when the synoptic situation is favorable - especially after the passage of a low pressure at the north of Terre Adélie. The dry air carried by a katabatic wind significantly influences the lower layers of the atmosphere at the coasts, notably through the sublimation of precipitation. Snowfall at DDU is mostly associated with the passage of a warm front of an extratropical cyclone transiting over the Southern Ocean (Jullien et al. [2020]). Dry katabatic winds sublimate a substantial part of the precipitation (Grazioli et al. [2017b]) especially during the pre-frontal and post-frontal phase of the precipitation event (Jullien et al. [2020]). As summer temperature can sometimes

1 exceed 0°C, rainfall occasionally occurs (Vignon et al. [2021]) especially when a strong blocking anticyclone form to
 2 the north east of the station. A study carried out by Grazioli et al. [2017a] over one year has shown that the annual
 3 precipitation amount at DDU would be between 740 and 989 mm. The evolution of the temperature and wind force
 4 variables recorded during the YOPP campaign all well as statistics are presented in the Figure 3. During the YOPP
 5 campaign, the daily average of the hourly maximum temperature have been 0.5°C with only 8 days of positive daily
 6 mean temperature. The daily average of the hourly minimum and mean temperatures have been respectively -4.6°C
 7 and -2.0°C. Over 92 days, the daily average of hourly maximum temperature remained below 0°C for 34 days and
 8 the daily average of hourly minimum temperature did not exceed -5°C for 38 days (see Figure 3). Most of the wind
 9 blowing at the station is easterly or south-easterly and ranges between 7 to 14 m.s⁻¹ (not shown). The daily average
 10 of the hourly mean wind speed and hourly instant wind speed during the campaign are 6 and 21 m.s⁻¹. The strength
 11 of the hourly gusts averaged over the day exceeded 28 m.s⁻¹ per hour for 25 days out of 92 days of the campaign.
 12
 13
 14

3.2 | Days with snowfall observed during the YOPP campaign



38 **FIGURE 4** a) Time serie of the surface snowfall measured by the snow gauge OTT PLUVIO2 during the YOPP period (red :
 39 days with intense snowfall, blue : days with medium snowfall, green : days with small and very small snowfall). b) Time serie of
 40 the vertical snowfall flux measured by the MRR during the YOPP period (white : no or negligible precipitation) and the surface
 41 snowfall measured by the snowgauge OTT PLUVIO2

42
 43 Considering the threshold mentioned above of 0.28mm per day, the snow gauge has detected 24 non-negligible days
 44 with snowfall during the 92-day campaign. The Figure 4 shows the daily time serie of the snowfall measured by the
 45 instrument at the surface. During the summer campaign, there were respectively 3, 2 and 19 days of high, medium
 46 and low or very low snowfall intensity. The time series of surface precipitation as well as that on the vertical show
 47 a drier period from the 25th (10/12/2018) to the 80th (03/02/2019) day of the period. The Figure 4 shows a very
 48
 49
 50
 51
 52
 53
 54
 55

good agreement between the occurrences observed by the MRR (at its first level) and those of the snow gauge.

4 | EVALUATION OF THE MODEL PRECIPITATION OCCURENCE AND AMOUNTS

TABLE 3 Scores (Bias, Probability Of Detection and Ratio of False Alarm) of model outputs for the occurrence of surface and vertical snowfall during the YOPP campaign respectively compared to observations. Green and red respectively indicates the best and worst score among all models

Model / Score	Surface				Vertical			
	BIAS	POD	FAR	HSS	BIAS	POD	FAR	HSS
ARPEGE-SH	1.78	0.94	0.47	0.57	1.05	0.87	0.17	0.74
ECMWF-OPER	2.11	1.00	0.53	0.51	1.10	0.89	0.19	0.74
LMDZ	1.50	0.78	0.48	0.51	1.13	0.81	0.29	0.57
MAR	1.28	0.89	0.30	0.72	1.20	0.86	0.29	0.60
ECMWF-ERA5	2.28	1.00	0.56	0.46	1.15	0.90	0.21	0.71
MERRA2	2.28	1.00	0.56	0.46	1.14	0.89	0.22	0.71

4.1 | At the surface

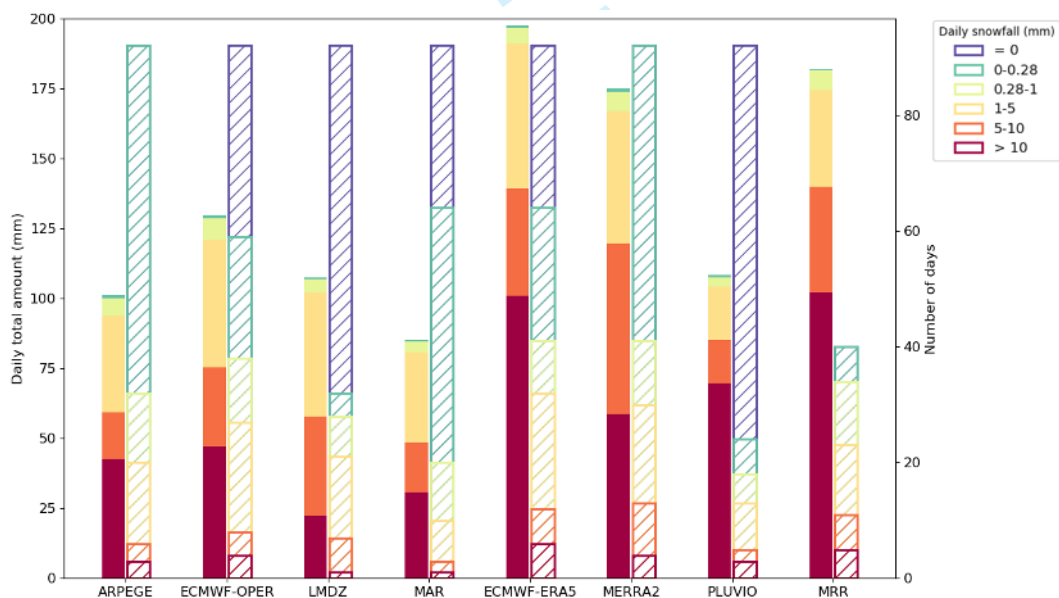


FIGURE 5 Left bars : Daily total amount of surface snowfall for model outputs and observations classified by daily surface snowfall amount classes (in mm). Right bars : Number of days classified by daily surface snowfall amount classes for model outputs and observations (for the MRR, there is no day with a null daily snowfall because no zero value is present in the dataset)

TABLE 4 Total surface accumulation in millimeters for model outputs and observations

	Total surface snowfall
ARPEGE-SH	101
ECMWF-OPER	130
LMDZ	125
MAR	85.1
ECMWF-ERA5	198
MERRA2	175
PLUVIO	109
MRR	182

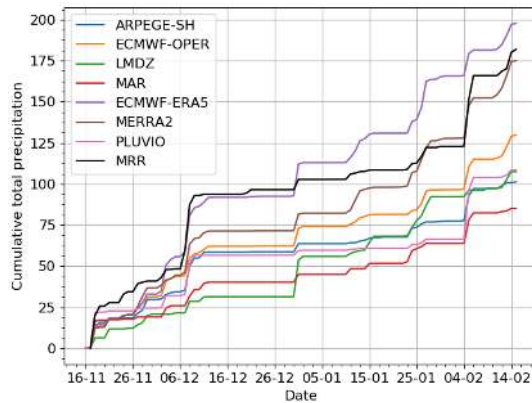


FIGURE 6 Time serie of the cumulative surface (or at the lowest available gate i.e at 300 m a.g.l for MRR) snowfall for model outputs and observations

At the surface, regarding precipitation amounts, the model outputs with best agreement with observations are those from ARPEGE-SH with a global underestimation of 7% of the total accumulation (see the Table 4) and LMDZ with an overestimation of 15%. MAR is underestimating it with an error of 24%. The two reanalyses are overestimating the quantity with larger errors : 61% for MERRA5 and 82% for ERA5. When considering days with snowfall by intensity class, LMDZ reproduces the best distribution of day types with the smallest standard deviation compared to surface observation data (not shown). The repartition of different contribution is illustrated in the Figure 5. ARPEGE and MERRA2 have the most dissimilar repartition from the snow gauge, especially due to a major overestimation of negligible snowfall daily amounts. All models do not represent days with exactly 0mm or with a negligible amount of snowfall (0-0.28mm/day) the same way. However we investigated days with little accumulation considering small (1-5mm/day) and very small (0.28-1mm/day) snowfall amounts : the analysis of the contribution of those days with snowfall shows that their occurrences are predominant, and that they are generally well represented in all the models. Regarding the total accumulation, the contribution of days with very weak snowfall is negligible (see Figure 5) and the major part of the overall surface snowfall originates from days with intense, and medium or small snowfall. The time serie of cumulated precipitation day by day - illustrated in the Figure 6 - for all the models and observations shows that reanalyses are well representing the days with intense snowfall but overestimate some medium and small ones. ARPEGE is generally underestimating all strong and medium days with snowfall, MAR overestimates the number of days with negligible snowfall and does not simulate enough intense one. Finally, ARPEGE, IFS and LMDZ do not always simulate intense and moderate daily snowfall amounts well, but the compensation for these errors leads to a total accumulation close to that of the snow gauge (see Table 4). The HSS value for the models is close but major differences between them are highlighted by the other scores (see Table 3) : ERA5, MERRA2 and IFS have a perfect POD and ARPEGE has also a very high value for this score which is most probably a result of optimal assimilation of observed standard variables at the surface (as temperature, wind speed and humidity) while the other models are merely nudged at boundaries. The time serie of the results of the comparison of the models to the snow gauge observations at the surface (see Figure 6) shows that ERA5, MERRA2 and IFS do not miss a day with snowfall at the surface during the YOPP campaign and ARPEGE only misses a single day with snowfall. ERA5, MERRA2 and IFS have higher bias and ratio of false alarm due to too many precipitating days. MAR and LMDZ have the lowest bias, slightly overestimating the number of days with snowfall. However, the higher number of missed days with snowfall of these

models contributes to lower values of POD. MAR has the lowest false alarm ratio because of its under-representation of the number of days with significant snowfall which may be due to too small intensities of snowfall events. MAR and LMDZ have the same missed days with snowfall (around the twentieth day of the campaign - see Figure 6).

4.2 | Along the vertical

TABLE 5 Cumulative maximum snowfall in the column during the YOPP campaign across all vertical levels for model outputs and MRR observations in millimeters

	Maximum snowfall in the column
ARPEGE-SH	209
ECMWF-OPER	203
LMDZ	263
MAR	182
ECMWF-ERA5	276
MERRA2	207
MRR	217

TABLE 6 Standard deviation of the vertical distribution of total snowfall during the YOPP campaign for model outputs in millimeters

	Standard deviation
ARPEGE-SH	9.67
ECMWF-OPER	11.67
LMDZ	24.69
MAR	49.41
ECMWF-ERA5	17.57
MERRA2	17.22

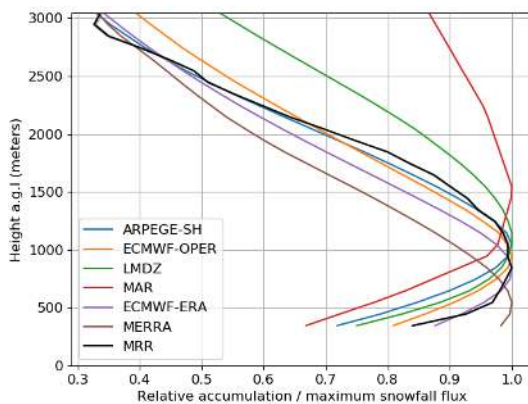


FIGURE 7 Vertical profiles of cumulative snowfall during the YOPP campaign normalized by the maximum snowfall flux in the column for model outputs and MRR observations

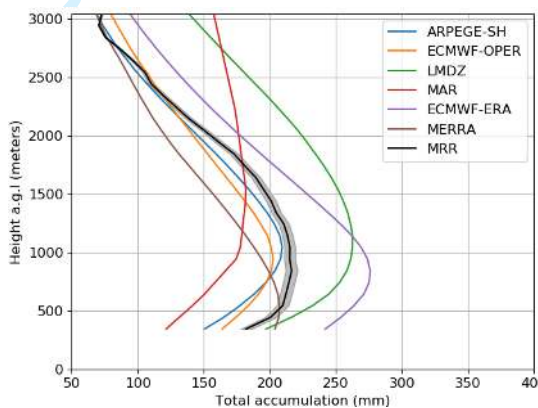


FIGURE 8 Vertical profiles of cumulative snowfall during the YOPP campaign for model outputs and MRR observations (with the centered uncertainty associated at each vertical level in grey color)

To perform the comparison between the MRR and the various model outputs, model data were vertically interpolated (using linear interpolation) on MRR levels. Along the vertical, each score is computed with the daily results of every level of the whole vertical column for each model. The analysis of the total precipitation flux profiles modeled during

1
2 the period (see Figures 7 and 8) shows that the result closest to the observation by the MRR is that of the ARPEGE
3 model, with the smallest standard deviation (computed with absolute values) compared to the observed profile. IFS
4 has closest values of quantity and height of the maximum value on the vertical compared to the MRR. Despite a
5 small bias in the value of surface snowfall - and all along the atmospheric column - the ERA5 reanalyses have a good
6 representation of the observed distribution as well as a close maximum snowfall flux on the vertical to the MRR
7 one. On the opposite the LMDZ and MAR models have the less consistent shape of vertical distribution with the
8 observation, respectively overestimating and underestimating maximum snowfall flux. In particular, the profiles with
9 relative snowfall values show that the sublimation of precipitation is too strong for all the models in the lower layers of
10 the atmosphere. It should be noted that the quantitative comparison of precipitation modeled by the different models
11 is done with the precipitation values obtained from the reflectivity measurements of the MRR. The uncertainty due to
12 the reflectivity-snowfall conversion ranges from 5% of the measured snowfall quantity at the bottom (lowest available
13 gate i.e at 300m a.g.l) to 2% at the top. Along the vertical, the scores of the different models were calculated only from
14 the occurrences of non precipitating days observed by the MRR, which reduces the number of model data processed
15 out of the totality available (see Table 3). All the models have a bias greater than 1 signifying a slight overestimation of
16 occurrence of days with snowfall. The ARPEGE and IFS models have the biases closest to 1 as well as high POD values
17 which indicates a good representation of snowfall occurrence. This interpretation is confirmed by the greatest values
18 of HSS. The two reanalyses MERRA2 and ERA5 have the best POD which can be explained by a higher number of
19 hits. However, they suffer from higher biases due to a higher number of excess predicted days with snowfall due to
20 an overestimation of the precipitation occurrences at DDU, concurring with the results of Jullien et al. [2020].
21
22
23

24 | 5 | DISCUSSION & CONCLUSION

25
26 Model-observation intercomparisons in the vertical are rare for precipitation : precipitation from models is generally
27 evaluated at ground level, because surface observations are the primary source of data available as a reference for
28 calibration or validation activities. Although accurate knowledge of average but also extremes surface precipitation
29 is our main goal, it is also important to verify that these precipitations are the result of the right physical processes.
30 The vertical profile offers the possibility to distinguish the altitudes where precipitation is formed by condensation
31 from those where it is sublimated, and thus to evaluate these two processes separately. Ideally a good model. Ideally
32 a good model will be able to represent it across the entire atmospheric column in terms of quantity and occurrence. It
33 is important for weather prediction that a model manages well the timing and therefore indirectly the precipitation
34 detection thresholds - because this is what defines whether precipitation occurs or not.
35
36

37 Despite the short time of available data, during the YOPP-SH SOP at DDU the comparison performed in this
38 study between models illustrates the potential of vertical information for model evaluation. YOPP-SH offers a good
39 opportunity to comparatively evaluate the performance of several meteorological and climate models and reanalyses
40 in both weather prediction and nudged mode in the polar environment. Here models have been evaluated at the DDU
41 YOPP-SH supersite during the YOPP austral summer special observing period, for their capabilities with respect to
42 precipitation thanks to ground-based radar data that are now available.
43

44 Even though we cannot indubitably ensure that better performances are due to data assimilation in these prod-
45 ucts, weather prediction models and reanalyses that benefits from the assimilation of observations better represent
46 the occurrences of precipitation. The ERA5 and MERRA2 reanalyses faithfully reproduce the chronology of surface
47 precipitation, allowing for example to characterize the water cycle in the region. However their positive bias must
48 be taken into account to make a surface precipitation climatology. The weather prediction models IFS and ARPEGE
49
50
51
52
53
54
55

1
2 are reliable in predicting accumulations of surface precipitation at DDU with less than 20% error on the accumulation
3 measured during the campaign. Good confidence can be also placed in the weather forecast models and the reanal-
4 yses to reproduce the precipitation profiles. The ARPEGE and IFS models have a correct vertical gradient, testifying
5 to their good representation of hydrometeores growth mechanisms. Contrary to the reanalyses, the MAR model un-
6 derestimate the total cumulative precipitation at the surface that can be explained by its less accurate representation
7 of the snowfall profile or by its underestimation of days with intense surface snowfall amounts. The LMDZ model
8 produces too much precipitation at altitude but this is compensated by strong sublimation towards the surface so
9 that it has a good estimate of surface accumulation. Regarding the precipitation occurrences, the calculated scores
10 indicate a better success of all the models on all the vertical levels compared to the surface only. This makes it possible
11 to account for the differences in the vertical distribution of precipitation. This vertical aspect is particularly critical for
12 DDU because of the evaporation near the surface but we can assume that this is also the case for all of Antarctica.

13
14 Even if the important information is what remains on the surface, in particular in the contribution to the calculation
15 of the SMB, the vertical is crucial to examine the deficiencies of a model in terms of representation of the processes -
16 for the Antarctic it is particularly important for the parameters of cold microphysics by which water vapor (advedted
17 from the ocean) condenses (forming clouds) and whose particles grow by different processes until they fall and become
18 precipitation. Since we show here how important the information along the vertical is to properly evaluate a model
19 in Antarctica, and that now we can obtain observations of precipitation profile from in-situ radar, we recommend to
20 deploy instruments of the same type as the MRR as well as favoring the passage of satellites capable of profiling
21 precipitation above the polar regions as CloudSat did and as EarthCare will soon do.

22 23 24 **acknowledgements**

25
26 The authors would like to dedicate this article to Chantal Claud, who unfortunately passed away while this work
27 was being carried out, in gratitude for her support and her experienced advice. This paper is a contribution to the
28 CALVA project supported by the French Polar Institute and to the YOPP, a flagship activity of the PPP, initiated by the
29 WWRP of the WMO. This research was carried out in the framework and with support of the French space agency
30 CNES/CNRS GDR EECLAT. CDA thanks FCT/MCTES for the financial support to CESAM (UIDP/50017/2020 and
31 UIDB/50017/2020) through national funds and support to project ATLACE (CIRCNA/CAC/0273/2019) funded by
32 FEDER, through COMPETE2020-Programa Operacional Competitividade e Internacionalização (POCI). We thank the
33 MAR team which make available the model outputs, as well agencies (F.R.S - FNRS, CÉCI, and the Walloon Region)
34 that provided computational resources for MAR simulations. MLR is supported by a grant of the Ecole Polytechnique
35 - IPP, Paris, France.

36 37 38 **authors contribution**

39
40 MLR carried out the data analysis and wrote the initial draft. CG is in charge of the program which carries out obser-
41 vations and supervises her thesis. EB carried out the ARPEGE simulations and contributed to the modeling aspects
42 of the article. VW performed the LMDZ simulations and CA the MAR ones. CDA provided the raw RADAR data
43 processing algorithm and contributed to the analysis of the results. All coauthors contributed to the writing.

44 45 46 **conflict of interest**

47
48 The authors declare that they have no conflict of interest.
49
50
51
52
53
54
55

references

- Agosta, C., Amory, C., Kittel, C., Orsi, A., Favier, V., Gallée, H., van den Broeke, M. R., Lenaerts, J. T. M., van Wessem, J. M., van de Berg, W. J. and Fettweis, X. (2019) Estimation of the antarctic surface mass balance using the regional climate model MAR (1979–2015) and identification of dominant processes. *The Cryosphere*, **13**, 281–296. URL: <https://tc.copernicus.org/articles/13/281/2019/>.
- Amory, C., Kittel, C., Le Toumelin, L., Agosta, C., Delhasse, A., Favier, V. and Fettweis, X. (2021) Performance of MAR (v3.11) in simulating the drifting-snow climate and surface mass balance of Adélie Land, East Antarctica. *Geoscientific Model Development*, **14**, 3487–3510. URL: <https://gmd.copernicus.org/articles/14/3487/2021/>.
- Bauer, P., Sandu, I., Magnusson, L., Mladek, R. and Fuentes, M. (2020) ECMWF global coupled atmosphere, ocean and sea-ice dataset for the year of polar prediction 2017–2020. *Scientific Data*, **7**.
- Boucher, O., Servonnat, J., Albright, A. L., Aumont, O., Balkanski, Y., Bastrikov, V., Bekki, S., Bonnet, R., Bony, S., Bopp, L., Braconnot, P., Brockmann, P., Cadule, P., Caubel, A., Cheruy, F., Codron, F., Cozic, A., Cugnet, D., D'Andrea, F., Davini, P., de Lavergne, C., Denvil, S., Deshayes, J., Devillers, M., Ducharne, A., Dufresne, J.-L., Dupont, E., Éthé, C., Fairhead, L., Falletti, L., Flavoni, S., Foujols, M.-A., Gardoll, S., Gastineau, G., Ghattas, J., Grandpeix, J.-Y., Guenet, B., Guez, Lionel, E., Guilyardi, E., Guimberteau, M., Hauglustaine, D., Hourdin, F., Idelkadi, A., Jousaume, S., Kageyama, M., Khodri, M., Krinner, G., Lebas, N., Levassasseur, G., Lévy, C., Li, L., Lott, F., Lurton, T., Luysaert, S., Madec, G., Madeleine, J.-B., Maignan, F., Marchand, M., Marti, O., Mellul, L., Meurdesoif, Y., Mignot, J., Musat, I., Ottlé, C., Peylin, P., Planton, Y., Polcher, J., Rio, C., Rochetin, N., Rousset, C., Sepulchre, P., Sima, A., Swingedouw, D., Thiéblemont, R., Traore, A. K., Vancoppenolle, M., Vial, J., Vialard, J., Viovy, N. and Vuichard, N. (2020) Presentation and evaluation of the IPSL-CM6A-LR climate model. *Journal of Advances in Modeling Earth Systems*, **12**, e2019MS002010. URL: <https://agupubs.onlinelibrary.wiley.com/doi/abs/10.1029/2019MS002010>. E2019MS002010 10.1029/2019MS002010.
- Bromwich, D. H. and Parish, T. R. (1998) Meteorology of the antarctic. *American Meteorological Society*, 175–200.
- Bromwich, D. H., Werner, K., Casati, B., Powers, J. G., Gorodetskaya, I. V., Massonnet, F., Vitale, V., Heinrich, V. J., Liggett, D., Arndt, S., Barja, B., Bazile, E., Carpentier, S., Carrasco, J. F., Choi, T., Choi, Y., Colwell, S. R., Cordero, R. R., Gervasi, M., Haiden, T., Hirasawa, N., Inoue, J., Jung, T., Kalesse, H., Kim, S.-J., Lazzara, M. A., Manning, K. W., Norris, K., Park, S.-J., Reid, P., Rigor, I., Rowe, P. M., Schmithusen, H., Seifert, P., Sun, Q., Uttal, T., Zannoni, M. and Zou, X. (2020) The Year of Polar Prediction in the Southern Hemisphere (YOPP-SH). *Bulletin of the American Meteorological Society*, **101**, E1653–E1676. URL: <https://journals.ametsoc.org/view/journals/bams/101/10/bamsD190255.xml>.
- Durán-Alarcón, C., Boudevillain, B., Genthon, C., Grazioli, J., Souverijns, N., van Lipzig, N. P. M., Gorodetskaya, I. V. and Berne, A. (2019) The vertical structure of precipitation at two stations in East Antarctica derived from micro rain radars. *The Cryosphere*, **13**, 247–264. URL: <https://www.the-cryosphere.net/13/247/2019/>.
- ECMWF (2017) Data archive of global meteorological fields from ECMWF integrated forecast system for the year of polar prediction. URL: <https://apps.ecmwf.int/datasets/data/yopp>.
- ECMWF (2021) *IFS Documentation CY47R3 - Part IV Physical processes*. No. 4 in IFS Documentation. ECMWF. URL: <https://www.ecmwf.int/node/20198>.
- Gallée, H. (1995) Simulation of the mesocyclonic activity in the ross sea, Antarctica. *Monthly Weather Review*, 2051–2069.
- Gelaro, R., McCarty, W., Suárez, M. J., Todling, R., Molod, A., Takacs, L., Randles, C. A., Darmenov, A., Bosilovich, M. G., Reichle, R., Wargan, K., Coy, L., Cullather, R., Draper, C., Akella, S., Buchard, V., Conaty, A., da Silva, A. M., Gu, W., Kim, G.-K., Koster, R., Lucchesi, R., Merkova, D., Nielsen, J. E., Partyka, G., Pawson, S., Putman, W., Rienecker, M., Schubert, S. D., Sienkiewicz, M. and Zhao, B. (2017) The Modern-Era Retrospective Analysis for Research and Applications, Version 2 (MERRA-2). *Journal of Climate*, **30**, 5419–5454. URL: <https://doi.org/10.1175/JCLI-D-16-0758.1>.
- Genthon, C., Berne, A., Grazioli, J., Durán Alarcón, C., Praz, C. and Boudevillain, B. (2018) Precipitation at Dumont d'Urville, Adélie Land, East Antarctica: the APRES3 field campaigns dataset. *Earth System Science Data*, **10**, 1605–1612. URL: <https://www.earth-syst-sci-data.net/10/1605/2018/>.

- 1
2 Genthon, C., Krinner, G. and Cosme, E. (2002) Free and laterally nudged antarctic climate of an atmospheric general circulation
3 model. *Monthly Weather Review*, **130**, 1601 – 1616. URL: [https://journals.ametsoc.org/view/journals/mwre/130/6/](https://journals.ametsoc.org/view/journals/mwre/130/6/1520-0493_2002_130_1601_fa1nac_2.0.co_2.xml)
4 [1520-0493_2002_130_1601_fa1nac_2.0.co_2.xml](https://journals.ametsoc.org/view/journals/mwre/130/6/1520-0493_2002_130_1601_fa1nac_2.0.co_2.xml).
- 5
6 GMAO (2015) MERRA-2 tavg3_3d_mst_ne: 3d,3-hourly,time-averaged,model-level edge,assimilation,moist processes diag-
7 nostics v5.12.4. *Tech. rep.*, Greenbelt, MD, USA, Goddard Earth Sciences Data and Information Services Center (GES
8 DISC). DOI: 10.5067/JRUZ3S3ZJ72 (accessed May 8, 2020).
- 9
10 Grazioli, J., Genthon, C., Boudevillain, B., Durán-Alarcón, C., Del Guasta, M., Madeleine, J.-B. and Berne, A. (2017a) Mea-
11 surements of precipitation in Dumont d'Urville, Adélie land, East Antarctica. *The Cryosphere*, **11**, 1797–1811. URL:
12 <https://www.the-cryosphere.net/11/1797/2017/>.
- 13
14 Grazioli, J., Madeleine, J.-B., Gallée, H., Forbes, R., Genthon, C., Krinner, G. and Berne, A. (2017b) Katabatic winds diminish
15 precipitation contribution to the antarctic ice mass balance. *Proceedings of the National Academy of Sciences*, **114**, 10858–
16 10863. URL: <https://www.pnas.org/content/114/41/10858>.
- 17
18 Hersbach, H., Bell, B., Berrisford, P., Hirahara, S., Horanyi, A., Muñoz-Sabater, J., Nicolas, J., Peubey, C., Radu, R., Schepers, D.,
19 Simmons, A., Soci, C., Abdalla, S., Abellan, X., Balsamo, G., Bechtold, P., Biavati, G., Bidlot, J., Bonavita, M., De Chiara, G.,
20 Dahlgren, P., Dee, D., Diamantakis, M., Dragani, R., Flemming, J., Forbes, R., Fuentes, M., Geer, A., Haimberger, L., Healy, S.,
21 Hogan, R., Holm, E., Janiskova, M., Keeley, S., Laloyaux, P., Lopez, P., Lupu, C., Radnoti, G., De Rosnay, P., Rozum, I.,
22 Vamborg, F., Villaume, S. and Thepaut, J.-N. (2020) The ERA5 global reanalysis. *Quarterly Journal of the Royal Meteorological*
23 *Society*, **146**, 1999–2049. URL: <https://rmets.onlinelibrary.wiley.com/doi/10.1002/qj.3803>.
- 24
25 Hourdin, F., Rio, C., Grandpeix, J.-Y., Madeleine, J.-B., Cheruy, F., Rochetin, N., Jam, A., Musat, I., Idelkadi, A., Fairhead, L.,
26 Fojouls, M.-A., Mellul, L., Traore, A.-K., Dufresne, J.-L., Boucher, O., Lefebvre, M.-P., Millour, E., Vignon, E., Jouhaud, J.,
27 Diallo, F. B., Lott, F., Gastineau, G., Caubel, A., Meurdesoif, Y. and Ghattas, J. (2020) LMDZ6A: The Atmospheric Component
28 of the IPSL Climate Model With Improved and Better Tuned Physics. *Journal of Advances in Modeling Earth Systems*, **12**,
29 e2019MS001892. URL: <https://hal.archives-ouvertes.fr/hal-02903162>.
- 30
31 Jullien, N., Vignon, E., Sprenger, M., Aemisegger, F. and Berne, A. (2020) Synoptic conditions and atmospheric moisture path-
32 ways associated with virga and precipitation over coastal Adélie Land in Antarctica. *The Cryosphere*, **14**, 1685–1702. URL:
33 <https://tc.copernicus.org/articles/14/1685/2020/>.
- 34
35 Kessler, E. (1995) On the continuity and distribution of water substance in atmospheric circulations. *Atmospheric Research*,
36 **38**, 109–145. URL: <https://www.sciencedirect.com/science/article/pii/016980959400090Z>.
- 37
38 Kittel, C., Amory, C., Agosta, C., Jourdain, N. C., Hofer, S., Delhasse, A., Doutreloup, S., Huot, P.-V., Lang, C., Fichet, T. and
39 Fettweis, X. (2021) Diverging future surface mass balance between the antarctic ice shelves and grounded ice sheet. *The*
40 *Cryosphere*, **15**, 1215–1236. URL: <https://tc.copernicus.org/articles/15/1215/2021/>.
- 41
42 Krinner, G., Beaumet, J., Favier, V., Déqué, M. and Brutel-Vuilmet, C. (2019) Empirical run-time bias correction for antarctic
43 regional climate projections with a stretched-grid AGCM. *Journal of Advances in Modeling Earth Systems*, **11**.
- 44
45 König-Langlo, G., King, J. C. and Pettré, P. (1998) Climatology of the three coastal antarctic stations Dumont d'Urville,
46 Neumayer, and Halley. *Journal of Geophysical Research: Atmospheres*, **103**, 10935–10946. URL: [https://agupubs.](https://agupubs.onlinelibrary.wiley.com/doi/abs/10.1029/97JD00527)
47 [onlinelibrary.wiley.com/doi/abs/10.1029/97JD00527](https://agupubs.onlinelibrary.wiley.com/doi/abs/10.1029/97JD00527).
- 48
49 Le Toumelin, L., Amory, C., Favier, V., Kittel, C., Hofer, S., Fettweis, X., Gallée, H. and Kayetha, V. (2021) Sensitivity of the
50 surface energy budget to drifting snow as simulated by MAR in coastal Adélie land, Antarctica. *The Cryosphere*, **15**, 3595–
51 3614. URL: <https://tc.copernicus.org/articles/15/3595/2021/>.
- 52
53 Lemonnier, F., Chemison, A., Krinner, G., Madeleine, J., Claud, C. and Genthon, C. (2021) Evaluation of coastal antarctic
54 precipitation in LMDZ6 global atmospheric model using ground-based radar observations. *Arctic and Antarctic Research*,
55 **67**, 147–164.

- 1
2 Lemonnier, F., Madeleine, J.-B., Claud, C., Palerme, C., Genthon, C., L'Ecuyer, T. and Wood, N. B. (2020) CloudSat-
3 inferred vertical structure of snowfall over the antarctic continent. *Journal of Geophysical Research: Atmospheres*, **125**,
4 e2019JD031399. URL: <https://agupubs.onlinelibrary.wiley.com/doi/abs/10.1029/2019JD031399>. E2019JD031399
5 10.1029/2019JD031399.
- 6 Maahn, M. and Kollias, P. (2012) Improved micro rain radar snow measurements using doppler spectra post-processing. *At-*
7 *mospheric Measurement Techniques*, **5**, 2661–2673. URL: <https://amt.copernicus.org/articles/5/2661/2012/>.
- 8 Madeleine, J.-B., Hourdin, F., Grandpeix, J.-Y., Rio, C., Dufresne, J.-L., Vignon, E., Boucher, O., Konsta, D., Cheruy, F., Musat, I.,
9 Idelkadi, A., Fairhead, L., Millour, E., Lefebvre, M.-P., Mellul, L., Rochetin, N., Lemonnier, F., Touzé-Peiffer, L. and Bonazzola,
10 M. (2020) Improved representation of clouds in the atmospheric component LMDZ6A of the IPSL-CM6A earth system
11 model. *Journal of Advances in Modeling Earth Systems*, **12**, e2020MS002046. URL: <https://agupubs.onlinelibrary.wiley.com/doi/abs/10.1029/2020MS002046>. E2020MS002046 10.1029/2020MS002046.
- 12
13 Pailleux, J., Geleyn, J.-F., Hamrud, M., Courtier, P., Thépaut, J.-N., Rabier, F., Andersson, E., Burridge, D., Simmons, A., Salmond,
14 D., El Khatib, R. and Fischer, C. (2014) Twenty-five years of IFS/ARPEGE. 22–30. URL: [https://www.ecmwf.int/node/](https://www.ecmwf.int/node/17335)
15 17335.
- 16
17 Palerme, C., Claud, C., Wood, N. B., L'Ecuyer, T. and Genthon, C. (2019) How does ground clutter affect CloudSat snowfall
18 retrievals over ice sheets? *IEEE Geoscience and Remote Sensing Letters*, **16**, 342–346.
- 19
20 Palerme, C., Genthon, C., Claud, C., Kay, J. E., Wood, N. B. and L'Ecuyer, T. (2017) Evaluation of current and projected antarctic
21 precipitation in CMIP5 models. *Climate Dynamics*, **48**, 225–239. URL: <https://doi.org/10.1007/s00382-016-3071-1>.
- 22
23 Palerme, C., Kay, J. E., Genthon, C., L'Ecuyer, T., Wood, N. B. and Claud, C. (2014) How much snow falls on the antarctic ice
24 sheet? *The Cryosphere*, **8**, 1577–1587. URL: <https://www.the-cryosphere.net/8/1577/2014/>.
- 25
26 Ricaud, P., Del Guasta, M., Bazile, E., Azouz, N., Lupi, A., Durand, P., Attié, J.-L., Veron, D., Guidard, V. and Grigioni, P. (2020)
27 Supercooled liquid water cloud observed, analysed, and modelled at the top of the planetary boundary layer above Dome-
28 C, antarctica. *Atmospheric Chemistry and Physics*, **20**, 4167–4191. URL: [https://acp.copernicus.org/articles/20/4167/](https://acp.copernicus.org/articles/20/4167/2020/)
29 2020/.
- 30
31 Roussel, M.-L., Lemonnier, F., Genthon, C. and Krinner, G. (2020) Brief communication: Evaluating antarctic precipitation in
32 ERA5 and CMIP6 against CloudSat observations. *The Cryosphere*, **14**, 2715–2727. URL: [https://tc.copernicus.org/](https://tc.copernicus.org/articles/14/2715/2020/)
33 [articles/14/2715/2020/](https://tc.copernicus.org/articles/14/2715/2020/).
- 34
35 USGS (2022) Antarctica overview map. URL: https://lima.usgs.gov/documents/LIMA_overview_map.pdf. Accessed Febru-
36 ary, 27 2022.
- 37
38 Vignon, E., Besic, N., Jullien, N., Gehring, J. and Berne, A. (2019a) Microphysics of snowfall over coastal East Antarctica
39 simulated by polar WRF and observed by radar. *Journal of Geophysical Research: Atmospheres*, **124**.
- 40
41 Vignon, E., Hourdin, F., Genthon, C., Van de Wiel, B. J. H., Gallée, H., Madeleine, J.-B. and Beaumet, J. (2018) Modeling the
42 Dynamics of the Atmospheric Boundary Layer Over the Antarctic Plateau With a General Circulation Model. *Journal of*
43 *Advances in Modeling Earth Systems*, **10**, 98–125. URL: <https://hal.sorbonne-universite.fr/hal-01727467>.
- 44
45 Vignon, E., Roussel, M.-L., Gorodetskaya, I. V., Genthon, C. and Berne, A. (2021) Present and future of rainfall in Antarctica.
46 *Geophysical Research Letters*, **48**, e2020GL092281.
- 47
48 Vignon, E., Traullé, O. and Berne, A. (2019b) On the fine vertical structure of the low troposphere over the coastal margins
49 of East Antarctica. *Atmospheric Chemistry and Physics*, **19**, 4659–4683. URL: [https://acp.copernicus.org/articles/19/](https://acp.copernicus.org/articles/19/4659/2019/)
50 4659/2019/.
- 51
52
53
54
55